De Iorio, Antonio, Grasso, Marzio, Penta, Francesco, Pucillo, Giovanni Pio, Rossi, Stefano and Testa, Mario (2018) On the ballast–sleeper interaction in the longitudinal and lateral directions. Proceedings of the Institution of Mechanical Engineers, Part F: Journal of Rail and Rapid Transit, 232(2), pp. 620-631.
 DOI: 10.1177/0954409716682629.

On the ballast-sleeper interaction in the longitudinal and lateral directions

Antonio De Iorio[1,4], Marzio Grasso[2], Francesco Penta[1], Giovanni Pio Pucillo[1], Stefano Rossi[3] and Mario Testa[3,4]

Abstract

In service, railway tracks must withstand transverse and longitudinal forces arising from running vehicles and thermal loads. The mechanical design adopting any of the track models available in the technical literature requires that the strength of the track is fully characterized. In this paper, the results of an experimental research activity on the sleeper ballast resistance along the lateral and the longitudinal directions are reported and discussed. In particular, the work is aimed at identifying the strength contributions offered by the base, the ballast between the sleepers, and the ballast shoulder to the global resistance of the track in the horizontal plane. These latter quantities were experimentally determined by means of an *ad hoc* system designed by the authors. Field tests were carried out on a series of track sections that were built to simulate scenarios in which the ballast was removed from the crib and/or the shoulder. The results of this study indicate that, as far as the scenarios here investigated are concerned, the strength percent contributions from the crib, the sleeper base and the shoulder are respectively equal to about 50%, 25%, and 25% in the lateral direction, and 60%, 30%, and 10% in the longitudinal one. Moreover, the comparison of the acquired data with literature results reveals that a detailed knowledge both of the testing conditions and the activated ballast failure mechanisms are needed in order to correctly use test data for design purpose.

Keywords: ballast resistance, railway track, track buckling, CWR track, superstructure, full scale test

[1] Department of Industrial Engineering, University of Naples Federico II, Naples, Italy
[2] School of Engineering and Technology, University of Hertfordshire, UK
[3] Technical Management/Technological and Experimental Standard/Superstructure, Rete Ferroviaria Italiana, Rome, Italy
[4] Now retired
Corresponding author:
Giovanni Pio Pucillo, Department of Industrial Engineering, University of Naples Federico II, P. le V. Tecchio 80, 80125, Naples, Italy

Email: gpucillo@unina.it

1. Introduction and background

Although Continuous Welded Rail (CWR) has solved many of the problems associated with tread surface discontinuities that occur in jointed tracks, the presence of compressive stresses in the rails caused by the solar heating and the longitudinal constraint action due to the ballast compel railroad engineers inspecting continuously the lines and carrying out the related maintenance operations to reduce the risk of thermal track buckling, a very complex phenomenon having often catastrophic consequences.

Researchers have focused their attention on the thermal buckling phenomenon for a long time and numerous experimental activities have been carried out until now, in order to identify analytical models and design practices that allow proper construction of the track against this failure mode.

Studies on thermal track buckling started in the first decades of the last century. Kerr in [1] critically surveyed most results of track buckling tests as well as the main theoretical analyses of track buckling published before the 1975. In most studies carried out since then in order to analyse the phenomenon in greater detail, an equivalent beam having the same cross section and rotational inertia as the real track [2--8] replaced the rail/sleeper structure. These beam models are quite intuitive but they cannot take into account the strong influence of the torsional stiffness of the fasteners nor the effects of missing ties and fasteners, being the beam continuously constrained to the ballast.

To overcome this latter limitation, Hengstum and Esveld [9] and El Ghazaly et al. [10] analysed the track equilibrium under thermal loading by 2D finite element (FE) method. For the same reason, Jackson et al. [11] proposed the rail tie model, a track finite element model built by super elements technique.

Since the real track buckling modes are often due to the interaction between lateral and torsional buckling, 3D models are thus necessary to study this interaction effect. A FE model of this kind was proposed by Lei and Feng [12]. Similar FE models were developed [13,14] in order to carry out sensitivity analyses of the ballast resistance and track irregularities on the stability of CWR.

Although the theoretical enquiries which have been carried out so far reached a very high complexity level, the reliability of the results of any analysis of the track behaviour is still strongly conditioned by the uncertainties about the ballast behaviour and the interactions of this latter with the track grate [13,15].

Until now, several researches aimed at measuring the ballast resistance have been carried out, among which it is worthy to highlight those conducted in USA [16--18], UK [19,20], Australia [21] as well the most popular study conducted by the European Rail Research Institute (ERRI) [22,23]. Data until now acquired were obtained from particular track configurations and, as a consequence, it is not possible to use them as a basis for quantitative predictions of the ballast behaviour in scenarios different from those from which they were derived. Moreover, most of them refer to the lateral

resistance only, disregarding the role the longitudinal stiffness has on the thermal buckling of a ballasted railway track [13,14,16]. Furthermore, the experimental analyses reported in literature do not cover all the aspects involved in the ballast response. Very often, the scheduled experimental activities were not completed. The tests were usually not repeated, when they were, the number of repetitions was quite low or in some cases fixed without a criterion. Sometimes, the reported experimental results are partially censored or data are referred to hypothetically uniform conditions even if, in general, it is known that the presence of singularities in the subgrade can greatly alter the ballast behaviour.

The testing methods currently adopted to measure the in service ballast resistance are very laborious and time consuming [24,25,26]. In order to tentatively overcome these limitations of the measurement practices, an analytical approach for the evaluation of the lateral resistance based on a continuous recording both of the forces applied by the tamping machine to the track and the corresponding track displacements was proposed in [27,28]. Unfortunately, experimental practices which allow the direct or indirect measurement of the different frictional contributions to the lateral track strength are still unknown.

The relative importance of the three main contributions to the lateral and longitudinal sliding resistance, namely the sleeper base, the crib, and the shoulder, depends on the track cross section geometry, ballast grain size and shape, grade of ballast compaction,

type of sleeper, type of rails, and type of subgrade. Also the mechanical loads acting on each sleeper exert a great influence. In particular, as reported in [29], the resistance offered by the base depends on the vertical load, while that related to the crib and shoulder is essentially related to the ballast internal friction and the volume of the grains interested by the sleepers movements [30]. Most of the studies carried out till now on the ballast strength contributions are essentially sensitivity analysis carried out by the FE method [to cite a few, 31 34]. In [22], literature data and ERRI tests results are analysed for the particular case of the unloaded track. Lateral strength is reported per sleeper and is defined as the peak lateral resistance within a deflection of about 20 mm. Details of the shoulder sizes, sleeper spacing, height of ballast and ballast mechanical properties are not specified. On the basis of these results, the ERRI suggested, as rule of thumb, that the base, the crib, and the shoulder contribute approximately 1/3 each to the lateral resistance. Le Pen and Powrie [30] quite recently discussed some test data and estimated for several shoulder geometry and sleeper loadings the relative contributions to the total sliding resistance of the base, crib and shoulder. In particular, the base contribution was related to the normal and moment loads using the Butterfield and Gottardi model [35], an approach that allows relating the ballast failure mechanisms to the differences in the contact pressure that arise on the surface between the ballast and the sleeper base. It is worth highlighting that the experimental data discussed in [30]

were produced in a laboratory by the single tie push test, an experimental methods that tends often to overestimate the ballast strength [22].

In order to fill in the gaps of the present scientific background on which the rules for design and maintenance of the CWR are based, further experimental investigations integrated with those which have been carried out until now are needed. More specifically, a specific testing program is necessary to characterize the ballast behaviour in a wide range of track configurations and, to obtain reliable results, a full field campaign would be preferable, since it allows reproducing testing conditions very close to the track service ones.

In this study, some experimental results obtained by tests carried out on track panels in the lateral and longitudinal directions are reported and critically discussed. This experimental activity aims at an in depth understanding of the relative importance of the three main contributions to the lateral and longitudinal sliding resistance, namely those offered by the crib, the shoulder and the sleeper base. It is part of a Research Project funded by RFI to study the stability of the continuous welded rail [26,36--38]. The main aims of the project were the ballast mechanical characterization in the widest possible number of service conditions (scenarios) and a new track model for studying the thermal buckling and post buckling track behaviour [13,36,37]. The experimental analysis of the longitudinal ballast contributions is a quite innovative aspect of this

work, since only one other study [25], to our knowledge, has specifically dealt with this problem on the base of in service ballast strength measurements.

From the comparison of data acquired by the authors with those from literature, interesting considerations can be drawn regarding the effects produced by the track geometry configurations and ballast conditions on the relative weight of the frictional contributions to the lateral strength of the track.

2. Field tests

The experimental data of the present paper were obtained from a testing campaign carried out in Traccia, near the Central Train Station in Naples, in an area provided by RFI (Italian Railway Infrastructure) during the Research Program previously mentioned.

The track panels to be tested were obtained from a single tangent track approximately 200 m long (Fig. 1) that was composed of 237 kg FSV35P concrete sleepers spaced at 0.6 m, and 60 kg/m UIC60 rail profiles. The FSV35P sleepers are 2.42 m long, and their cross section at the sleeper ends has a base of 280 mm and an height of 190 mm. The ballast height under the sleepers was about 40 cm, while the ballast shoulder width was 55 cm.

FIGURE #1

Figure 1. Tests field of Traccia in Naples.

From the track line, seven scenarios were developed. They are also sketched in the testing plan shown in Fig. 2. In particular, 4 scenarios were prepared for lateral pull tests, while 3 scenarios were for longitudinal pull tests. Both the ballast distribution around the sleepers and the number of sleepers were different in each scenario.

FIGURE #2

Figure 2. Track sectioning scheme to obtain test scenarios.

2.1 Site preparation

By means of a tamping machine, the operations of lining, levelling and tamping of the tangent track were initially performed for a length of about 300 m. Afterwards, in order to reduce stresses in the rails of the track from which the panels to be tested were to be obtained, the 200 m track segment was isolated by cutting the rails by a disk saw and creating a clearance of about 1.0 cm.

Then, each test panel was identified along the track. Each end was marked (by spray paint) on the rails heads; similarly, several point markers were sketched on the web of the two rails to identify the positions of the holes for the rod of the testing fixture.

After ballast compaction by a DTS (dynamic track stabilizer), all fastener systems were unscrewed and re tightened in order to perform rail normalization. Finally, the short

track panels were cut and drilled, removing the ballast where required (between sleepers and/or on the ballast shoulder). As shown in Fig. 2, each track panel was separated by the adjacent ones by two "inactive sleepers" in order to avoid interactions between the failure wedges of the ballast shoulders. The contact pressure distributions between the sleeper and the ballast bed are different when the track is loaded along either the longitudinal or the lateral direction, resulting in a different contribution of the base to the total resistance. For this reason it has been experimentally identified along both directions.

The tested scenarios are as follow:

a) for lateral pull tests:

- 4 sleepers surrounded by ballast up to the upper surface level (namely with crib and shoulders BBB);
- 4 sleepers and ballast removed from the crib (BCB);
- 4 sleepers and shoulder swept down to the sleeper base (BBU);
- 4 sleepers and ballast removed from the sides (BCU);

b) for longitudinal pull tests:

- 6 sleepers surrounded by ballast up to the upper surface level (BBB);
- 6 sleepers and shoulder swept down to the sleeper base (BBU);
- 6 sleepers and ballast removed from the sides (BCU).

2.2 Equipment and Test system

All tests were carried out using two or four loading lines, for the longitudinal and lateral pull tests, respectively. A testing system, which was specifically designed to carry out all the research activities scheduled in the aformentioned research project, was used.

In particular, the system is modular and is configurable up to a maximum of five loading lines operating simultaneously. Each loading lines (Fig. 3a) is composed by: an electromechanical actuator; one or more load cells (depending on the test configuration); a displacement transducer. A closed loop displacement control operates the actuators by means of a programmable digital controller. Both the digital control system and the data acquisition unit were mounted on a hand sliding truck that allowed easy moving and repositioning of all the testing equipments along the track during the scheduled activities (Fig. 3b). The experimental apparatus have been fully described by the authors in a previous paper [26].

FIGURE #3LR

Figure 3. Test system: the series of actuators (a) and the control and acquisition unit (b).

Due to the differences between the previous experimental campaign [26] and that reported in this paper, new interfaces to connect the loading system and the track were

needed. In particular, at the present testing site there was only a single track hence a railroad loader was used as fixed constraint. However, the loader shape did not provide many coupling options, which were at the same time simple, cheap and quick to be implemented. For this reason, the central point on the front axle (Fig. 4) was chosen to constrain the loading lines. Due to this choice, a bespoke fixture which was at the same time easy to assemble and disassemble, versatile, light and sufficiently stiff and stable was designed. The result of this design activity is the structure shown in Fig. 4. The system allows to transfer the load, which is applied by the actuators along different loading lines, to a single point on the test article as well as to the constraining point. The main feature of this system is the possibility to connect chains, cables or ropes using off the shelf hooks. In addition, it is possible to quickly split it up, being assembled using only bolts, and move from one site to another.

FIGURE #4

Figure 4. Loads transferring structure hooked to a railroad loader.

3. Experimental Results

Using the loading system previously described, the scheduled tests were carried out. The tests, which have been performed under displacement control, were carried out in order to identify the characteristic curve under specific track conditions. With this aim, regardless the plasticity and the failure condition of the ballast bed, each tests was

carried out until the displacement value was at least 80 mm. This would ensure that the characteristic curve experimentally obtained could be used to set up either a numerical or an analytical model through which the post buckling behaviour of the track under thermal buckling could be studied. Moreover, some scenarios have been tested further pulling the panel above 80 mm. In some cases, before the end of the test, the panel has been unloaded and reloaded. This diversion from the maximum displacement above defined is due to the possibility either gathering further data regarding the variation in stiffness after reaching the ballast plasticity or to assess the variation in the resistance after track unloading.

The applied load was recorded during the lateral pull tests along the longitudinal axis of each sleeper, whilst during the longitudinal pull tests the force values were measured along the longitudinal axes of the two rails of the track panel. The corresponding displacements values were recorded during the tests along the above described loading lines.

Signals of all the sensors of the experimental setup were acquired and processed in real time during the tests, in order to directly correlate the acquired data with the test parameters [26].

For each scenario, the instantaneous averages of both the loads applied to the sleepers and of the corresponding (sleepers) displacements were computed in real time during

the test, in order to have an average load displacement characteristic curve that was representative of the behaviour of all the sleepers of the tested scenario.

3.1 Transversal resistance tests on short tracks

Lateral resistance tests were performed on 4 track panels, each one of them composed by 4 sleepers and characterized by the presence (B) or not of the ballast between sleepers (C) and/or in correspondence of the shoulder (U), as shown in Figs. 5--8.

FIGURE #5

Figure 5. Test on BBB scenario (with ballast shoulder and ballast crib).

FIGURE #6

Figure 6. Test on BCB scenario (without ballast crib - C).

FIGURE #7

Figure 7. Test on BBU scenario (without ballast shoulder - U).

FIGURE #8

Figure 8. Test on BCU scenario (without ballast crib, C, and at sleepers ends, U).

The characteristic load displacement curves obtained averaging the curves obtained in each test are reported in Fig. 9. The difference in resistance values offered by the ballast in the four test configurations is self explanatory.

Such difference is also quantifiable in terms of the load peak values reported in Tab. 1. Moreover, on the basis of these values, the percentage contributions offered by the base, the crib and the shoulder were estimated (Tab. 2).

FIGURE #9

Figure 9. Lateral pull tests: load-displacement curves.

TABLE #1

Table 1. Measured transversal resistance peak values per sleeper (F_{Transv} *Isleeper*) and per track unit length (F_{Transv} *Ilinear metre*).

TABLE #2

Table 2. Contributions of the crib, the shoulder and the under sleeper ballast to the transversal resistance.

The percentage contribution of the sleeper base was estimated as the ratio between the value measured in the BCU scenario (ballast removed from the shoulder and from the crib) and the one measured in the BBB scenario. The contributions from the shoulder and the crib were obtained combining the results obtained from four scenarios, namely BBB, BCB, BCU, BBU, according to two different set.

The first set of scenarios is BBB/BCB/BCU. The contribution due to the ballast on the lateral sleeper surfaces can be estimated by subtracting from the value of the lateral resistance measured in the BBB scenario, the corresponding value measured in the BCB scenario (second row of Tab. 2). The contribution offered by the shoulder can be identified using a similar procedure: the lateral resistance value of the BCU scenario is subtracted from the value of the lateral resistance measured in the BCB scenario (fifth row of Tab. 2).

The second set of scenarios is BBB/BBU/BCU. The values of the lateral resistance can be computed following a similar procedure. The corresponding results are reported in the third and fourth rows of Tab. 2.

The percentage values estimated utilising the BBB BCB BCU and the BBB BBU BCU set of three scenarios respectively are reported in the third and fourth column of Tab. 2. The two adopted methodologies lead to very close values of the contribution offered by the shoulder and crib ballast. Moreover, although the ballast was removed either with mechanical devices in some scenarios, or manually stone by stone in others, the values related to the different contributions are very close.

3.2 Longitudinal resistance tests

Longitudinal resistance tests were performed on 3 track panels. Each of them contains 6 sleepers. As in the lateral tests, the ballast configurations of these panels were different, since the scenarios were made with or without shoulder and/or crib ballast.

To be able to perform these tests without interfering with the adjacent scenarios, all the sleeper located between the first track panel to be tested and the movable ends of the actuators was removed (Fig. 10). Moreover, two rail sections about 1.2 m long were removed, to insert two actuators of the testing system between the panel under testing and the constraining points (Fig. 10).

FIGURE #10

Figure 10. First longitudinal pull test: details of the actuators and their connections to the rails.

For the second test, the rails of the first scenario were removed to connect the panel to be tested to the actuators constrained to the fixed track by means of two chains (Fig. 11).

FIGURE #11

Figure 11. Second longitudinal pull test: detail of actuators linkage to the short track panel.

The third test was carried out in a similar way as the second one. During one of the three tests the panel was unloaded and reloaded in order to verify the path followed by the load displacement curve and assess the stiffness of the track. A further assessment refers to the force value reached when the panel is reloaded since it must be the same as it was before unloading.

The characteristic curves obtained from these tests, representing the average ballast resistance (per unit track length) as a function of the track displacement, are shown in Fig. 12. The peak values reached in each test are also reported in Tab. 3.

Based on the data obtained from these tests, the percentage contributions to the global longitudinal resistance offered by the base, the crib, and the shoulder were estimated (see Tab. 4) using an approach similar to the one previously adopted for the transversal strengths.

FIGURE #12

Figure 12. Longitudinal pull tests: load-displacement curves.

TABLE #3

Table 3. Measured longitudinal resistance peak values per sleeper (F_{Long} *Isleeper*) and per track unit length (F_{Long} *Ilinear metre*).

TABLE #4

Table 4. Contributions of the crib, the shoulder and the under sleeper ballast to the longitudinal resistance.

Discussion

The obtained results, when compared with those from the literature, well highlight the strong influence exerted both by the measuring method, the corresponding equipment adopted for the investigations and the specific ballast conditions of the test site on the scatter of the experimental data.

In Tab. 5, for example, the peak values for unloaded tracks of the ballast transversal resistance acquired during the tests on the BBB track panel and those of a previous testing campaign carried out on similar scenarios [36] (where the RFI 230 ties were used instead of the FSV35P ties adopted in the scenarios of the present paper) are reported. They give an idea of the aforementioned scatter. The evident differences between the two set of strength values should dissuade anyone from using literature data lacking of precise information about the reference scenario and the adopted experimental practice.

However, neither the scatter quantification nor the analysis of its main sources are the central purpose of the present work. Instead, the presented experimental activity has been carried out essentially in order to collect data by which the individual strength

contributions from the crib, the shoulder, and the under sleeper ballast to the global resistance of the track in the horizontal plane can be evaluated and to generalize the obtained results to scenarios similar to the tested ones.

Two other comparisons with data taken from the literature are synthesized in Tables 6 and 7, where the lateral and longitudinal percent resistance contribution values of track panels tested in full field conditions [25] are compared with those obtained in the present study, and in Table 6, where the lateral contributions obtained in laboratory with the STPT technique [30] are compared with field data from DCPPT technique utilized in this study.

In [25], as expected, the contributions are quite different, due to the different geometrical parameters of the tracks, the different ballast type and grading curve.

TABLE #5

Table 5. Measured lateral resistance peak values.

TABLE #6

Table 6. Comparison of the contributions to lateral resistance with those of ERRI [25J and those of Le Pen and Powrie [30J.

TABLE #7

Table 7. Comparison of the contributions to longitudinal resistance with those of ERRI [25J.

The differences observed in the crib resistance contribution can be explained in terms of the failure mechanism. Crib resistance is essentially related to the slip energy dissipated by friction, either on the sides of the sleeper or on a slip surface level with the base of the sleepers within the ballast, according to the failure mechanism that offers the lesser resistance [30]. In our case, the first mechanism was observed, whereas in [25] no details are given about this aspect, which once again highlights the need of a detailed description both of the testing condition, and of the experimental observations of the failure mechanisms that wakes up when the critical conditions are attained. As in the case of crib ballast failure, in fact, if the experimental test field is made of poor ballast materials, internal ballast failure due to low internal friction coefficient will probably occur, which in turn would erroneously underestimate the sleeper ballast strength if for in service tracks more refined ballast materials are adopted.

In [30], where the testing condition were representative of freshly laid ballast, the ratio *LIV*, where *L* is the peak resistance of the base contribution in the lateral direction and *V* is the vertical load on the sleeper, attains the mean value of about 0.55 (see Table 6). For the track section considered in this study (237 kg FSV35P type sleepers spaced of 0.6 m, and 60 kg/m UIC60 rails), the weight of track per sleeper is *V* ::: 3140 N (2324 +

720 + weight of fasteners), whereas the peak value of the base contribution, L, was experimentally found to be equal to 1599.3 N (see Tables 1 and 6); this lead to L/V ::: 0.51, which is only about 7.5% smaller than the value reported in [30].

Also for the crib resistance a quite good agreement with the results of [30] can be appreciated (see second row of Table 6), being only about 5.4% the percent difference between results from [30] and the value we have measured. Moreover, this value further reduces if we calculate the crib contribution with the same procedure reported in [30] (we did it in two ways in subsection 3.1, as shown in the second and third row of Table 2, and the value of 2775.3 N reported in the second row of Table 6 is the mean value obtained by averaging the results of the two methods), namely by subtracting the BCU curve (only base contribution, fourth row of Table 1) from that obtained during the BBU test (base and crib contributions, third row of Table 1); in this case, in fact, a value of 2942.1 N is found, as reported in the third row of Table 2, which corresponds to a 0.2% only difference with respect to the results of [30]. Moreover, if we multiply this value by the ratio between the lengths of the sleepers utilized, respectively, in [30] and in this study, namely 2.5/2.42 = 1.03 (being 2.5 m the length of the sleeper utilized in [30] and 2.42 m that of this study), a crib resistance of 2942.1x1.03 ::: 3030 N is obtained, which is yet in good agreement (with a difference of 3%) with the value of 2935 N found in [30].

For the shoulder contribution, instead, the results obtained in [30] are about 32% higher than those of the present study, as shown in the second row of Table 6. As done above, this difference reduces if we consider the same procedure adopted in [30], namely by subtracting the BCU curve (fourth row of Table 1) from that obtained during the BCB test (base and shoulder contributions, second row of Table 1); following this method, a shoulder resistance of 1672 N is found (see fifth row of Table 2), which is about 25% smaller than the value found in [30]. However, if it is assumed that shoulder failure mechanism depends on the extension of ballast failure wedges, and that these areas are proportional with a same factor to the cross section perimeter of the sleeper end face, it seems correct, for data comparison with [30], to further multiply the above value by the ratio of cross section perimeters, $ll_{LP\text{-}P}/ll_{ts}$, where $ll_{LP\text{-}P}$ = 2x(29+21) = 100 cm (see Table 7 in [30]) and ll_{ts} = 2x(28+19) = 94 cm (see section 3) are, respectively, the cross section perimeter of the sleeper end face utilized by Le Pen and Powrie [30] and that of this study; following this approach, a value of 1779 N is obtained, which is about 20% smaller than the value found in [30].

Concerning the differences observed in the shoulder contributions, it is worthwhile to observe also that the adopted experimental practice may have a strong influence on the value of the shoulder strength. When tests are carried out according to the single tie push test (STPT), as done in [30], shoulder resistance is usually higher than that obtained by pull tests on cut panels containing several sleepers [15,23]. This is probably

due to the interactions between the different ballast failure wedges of adjacent sleepers. Both the experimental and numerical studies show that the shoulder resistance contribution depends strongly on the shoulder width, whilst results related to the effects of the shoulder height are controversial. In example, numerical results reported in [31] show that an increase in height of a ballast shoulder will increase the initial stiffness of the ballast, but has no influence on the peak resistance. Conversely, shoulder resistance curves experimentally obtained by Le Pen and Powrie [30] pointed out that the resistance peak value is higher as greater is the shoulder height.

Conclusions

During the numerical and experimental activities on the thermal stability of the continuous welded rail track, particular types of field tests for the measurement of the contributions offered by the ballast surrounding the sleeper to the track resistance in the lateral and longitudinal directions were carried out. Although longitudinal strength is a key factor for thermal track buckling phenomenon, there is limited literature in terms of base, crib, and shoulder contributions to global resistance.

For the sleeper type and spacing of this study, with ballast in loose tamped conditions, it was found that, for unloaded track:

- the contributions of crib, base, and shoulder are, respectively, about 50%, 25%, and 25% of the total lateral resistance;

- the contributions of crib, base, and shoulder are, respectively, about 60%, 30%, and 10% of the total longitudinal resistance.

Comparison of the lateral contributions with detailed STPT laboratory data taken from literature shows a good agreement, with the only exception of the shoulder, which was found smaller in the tests of this study. This is consistent with literature findings, being the results of the STPT technique affected by the border effects due adjacent sleepers.

Other comparisons with literature also highlighted the need of detailed description both of the testing condition, and of the experimental observations of the failure mechanisms that wakes up when the critical conditions are attained. For these reasons, the use of experimental results from scenarios that do not reproduce precisely actual track conditions, or that are not fully detailed, has to be avoided.

Acknowledgments

The authors wish to thank Stefano Lisi of RFI (Rome), the Regional Direction of RFI (Naples), and Giuseppe Farneti of Italcertifer (Rome), for their valuable advices and supports on this study.

References

[1] Kerr AD. Lateral Buckling of Railroad Tracks due to Constrained Thermal Expansions A Critical Survey. In: AD Kerr (ed) *Railroad Track Mechanics & Technology, Proceeding of a Symposium Held at Princeton University, April 21-23 1975*. Pergamon Press, 1978, pp.141-169.

[2] Kerr AD and Zarembski AM. The Response Equations for a Cross Tie Track. *Acta Mechanica* 1981; 40: 253-76.
[3] Grissom GT and Kerr AD. Analysis of lateral track buckling using new frame type equations. *International Journal of Mechanical Sciences* 2006; 48: 21-32.
[4] Kish A, Samavedam G and Jeong D. Influence of vehicle induced loads on the lateral stability of CWR track. Report no. DOT/FRA/ORD 85/03, Department of Transportation, Federal Railroad Administration, Washington, US, 1985.
[5] Samavedam G. Buckling and post buckling analysis of CWR in the lateral plane. Technical Note no. TN TS 34, British Railways Board, R&D Division, 1979.
[6] Samavedam G, Kish A and Jeong D. Parametric studies on lateral stability of welded rail track. Report no. DOT/FRA/ORD 83/07, Washington, US, 1983.
[7] Samavedam G, Kish A, Purple A and Schoengart J. Parametric analysis and safety concepts of CWR track buckling. Report no. DOT/FRA/ORD 93/26, Washington, US, 1993.
[8] Martinez IN, Sanchis IV, Fernandez PM and Franco RI. Analytical model for predicting the buckling load of continuous welded rail tracks. *Proc IMechE Part F: Journal of Rail and Rapid Transit* 2014; 229(5): 542-552.
[9] Esveld C and Hengstum LA. Track stability in tight curves. *Rail Int* 1988; 12: 15-20.
[10] El Ghazaly HA, Sherbourne AN and Arbabi F. Strength and stability of railway tracks - II. Deterministic, finite element stability analysis. *Comput Struct* 1991; 39(1/2): 23-45.
[11] Jackson JE, Bauld NR, Ramesh MS and Menon SC. A superelement for lateral track deformation. In: *Applied Mechanics Rail Transportation Symposium - 1988.* Chicago, US, 27 November-2 December 1988, pp.7-18.
[12] Lei X and Feng Q. Analysis of stability of continuously welded rail track with finite elements. *Proc IMechE Part F: Journal of Rail and Rapid Transit* 2004; 218(3): 225 233.
[13] Pucillo GP. Thermal buckling and post buckling behaviour of continuous welded rail track. *Veh Syst Dyn* 2016; 54(12): 1785 1807.
[14] Lim NH, Han SY, Han TH, Kang YJ. Parametric study on stability of continuous welded rail track Ballast resistance and track irregularity. *Steel Structures* 2008; 8: 171-181.
[15] Bae HU, Choi JY, Moon J and Lim NH. Development of a probabilistic buckling analysis scheme for continuous welded rail track. *Proc IMechE Part F: Journal of Rail and Rapid Transit* 2016; 230(3): 747-758.
[16] Kish A and Samavedam G. Track Buckling Prevention: Theory, Safety Concepts, and Applications. Report no. DOT/FRA/ORD 13/16, Department of Transportation, Federal Railroad Administration, Washington, US, 2013.
[17] Jeong DY. Analyses for Lateral Deflection of Railroad Track Under Quasi Static Loading. In: *Proceedings of the ASME 2013 Rail Transportation Division Fall Technical Conference*. Altoona, Pennsylvania, USA, 15 17 October 2013, paper no. RTDF2013 4710, pp.1 10. American Society of Mechanical Engineers.
[18] Kish A, Samavedam G and Wormley D. Fundamentals of track lateral shift for high speed rail applications. In: *ERRI Interactive Conference on Cost Effectiveness and Safety Aspects of Railway Track*, Paris, France, 8 9 December 1998, Federal Railroad Administration.
[19] Sinclair JC. Checking rail condition. Report, British Rail Research, Derby, UK, 1996.
[20] Shrubsall PR and Webber PJ. Verse; non destructive stress free temperature measurement of CWR. *Rail Engineering International* 2001; 30(4): 3-6.

[21] Wu Y, Rasul MG, Powell J et al. Rail temperature prediction model. In: *CORE 2012: Global Perspectives; Conference on Railway Engineering* (eds. M. Dhanasekar, T. Constable and D. Schonfeld), Brisbane, Australia, 10 12 September 2012, pp.81 90. Canberra, Australia: The Railway Technical Society of Australasia.

[22] ERRI Committee D202. Improved knowledge of forces in CWR track (including switches). Report no. 2, Review of Existing Experimental Work in Behaviour of CWR Track, European Rail Research Institute, Utrecht, 1995.

[23] ERRI Committee D202. Improved knowledge of forces in CWR track (including switches). Report no. 3, Theory of CWR Track Stability, European Rail Research Institute, Utrecht, 1995.

[24] Samavedam G, Kanaan A, Pietrak J, Kish A, Sluz A. Wood tie track resistance characterization and correlations study. Report no. DOT/FRA/ORD 94/07, 1995.

[25] ERRI D202/DT 363. Improved knowledge of forces in CWR track (including switches): Determination of lateral and longitudinal ballast resistance of a railway track by experimental tests. Report, European Rail Research Institute, Utrecht, 1997.

[26] De Iorio A, Grasso M, Penta F, Pucillo GP and Rosiello V. Transverse strength of railway tracks: part 2. Test system for ballast resistance in line measurement. *Frattura ed Integrita Strutturale* 2014; 30: 578-592.

[27] Koc W, Wilk A, Chrostowski P and Grulkowski S. Tests on lateral resistance in railway tracks during the operation of a tamping machine. *Proc IMechE Part F: Journal of Rail and Rapid Transit* 2011; 225(3): 325-340.

[28] Koc W and Wilk A. Investigations of methods to measure longitudinal forces in continuous welded rail tracks using the tamping machine. *Proc IMechE Part F: Journal of Rail and Rapid Transit* 2009; 223(1): 61-73.

[29] Zakeri JA and Barati M. Utilizing the track panel displacement method for estimating vertical load effects on the lateral resistance of continuously welded railway track. *Proc IMechE Part F: Journal of Rail and Rapid Transit* 2015; 229(3): 262-267.

[30] Le Pen LM and Powrie W. Contribution of Base, Crib, and Shoulder Ballast to the Lateral Sliding Resistance of Railway Track: A Geotechnical Perspective. *Proc IMechE Part F: Journal of Rail and Rapid Transit* 2011; 225(2): 113-128.

[31] Kabo E. A numerical study of the lateral ballast resistance in railway tracks. *Proc IMechE Part F: Journal of Rail and Rapid Transit* 2006; 220(4): 425-433.

[32] Zakeri JA, Esmaeili M, Kasraei A and Bakhtiary A. A numerical investigation on the lateral resistance of frictional sleepers in ballasted railway tracks. *Proc IMechE Part F: Journal of Rail and Rapid Transit* 2016; 230(2): 440-449.

[33] Montalban DL, Real HJI, Zamorano C, Real HT. Design of a new high lateral resistance sleeper and performance comparison with conventional sleepers in a curved railway track by means of finite element models. *Latin American Journal of Solids and Structures* 2014; 11(7): 1238-1250.

[34] Esmaeili M, Khodaverdian A, Neyestanaki HK, Nazari S. (2016). Investigating the effect of nailed sleepers on increasing the lateral resistance of ballasted track. *Computers and Geotechnics* 2016; 71: 1-11.

[35] Gottardi G, Butterfield R. On the bearing capacity of surface footings on sand under general planar load. *Soils and Foundations* 1993; 33(3): 68-79.

[36] De Iorio A, Grasso M, Penta F, Pinto P, Pucillo GP et al. Transverse strength of railway tracks: part 1. Planning and experimental setup. *Frattura ed Integrita Strutturale* 2014; 30: 478-485.

[37] Rete Ferroviaria Italiana (RFI). Technical Specification, Rome, Italy, June 2008.

[38] De Iorio A, Grasso M, Penta F, Pucillo GP, Rosiello V et al. Transverse Strength of Railway Tracks: part 3. Multiple scenarios test field. *Frattura ed Integrita Strutturale* 2014; 30:593-601.

Figure 1. Tests field of Traccia in Naples.
FIGURE #1
99x69mm (300 x 300 DPI)

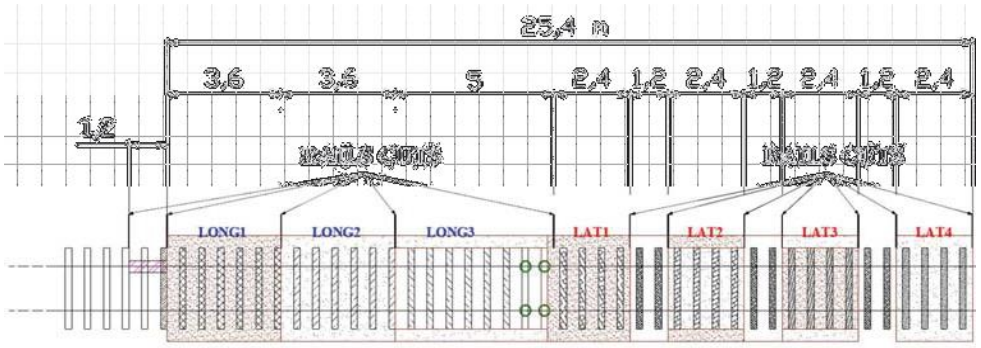

Figure 2. Track sectioning scheme to obtain test scenarios.
FIGURE #2
132x49mm (300 x 300 DPI)

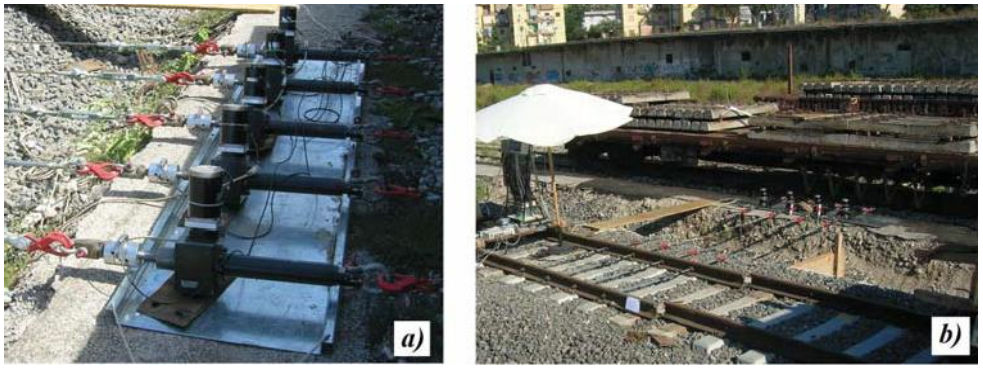

Figure 3. Test system: the series of actuators (a) and the control and acquisition unit (b).
FIGURE #3LR
973x360mm (96 x 96 DPI)

Figure 4. Loads transferring structure hooked to a railroad loader.
FIGURE #4
219x164mm (300 x 300 DPI)

Figure 5. Test on BBB scenario (with ballast shoulder and ballast crib).
FIGURE #5
219x164mm (300 x 300 DPI)

Figure 6. Test on BCB scenario (without ballast crib - C).
FIGURE #6
200x126mm (300 x 300 DPI)

Figure 7. Test on BBU scenario (without ballast shoulder - U).
FIGURE #7
218x113mm (300 x 300 DPI)

Figure 8. Test on BCU scenario (without ballast crib, C, and at sleepers ends, U).
FIGURE #8
219x164mm (300 x 300 DPI)

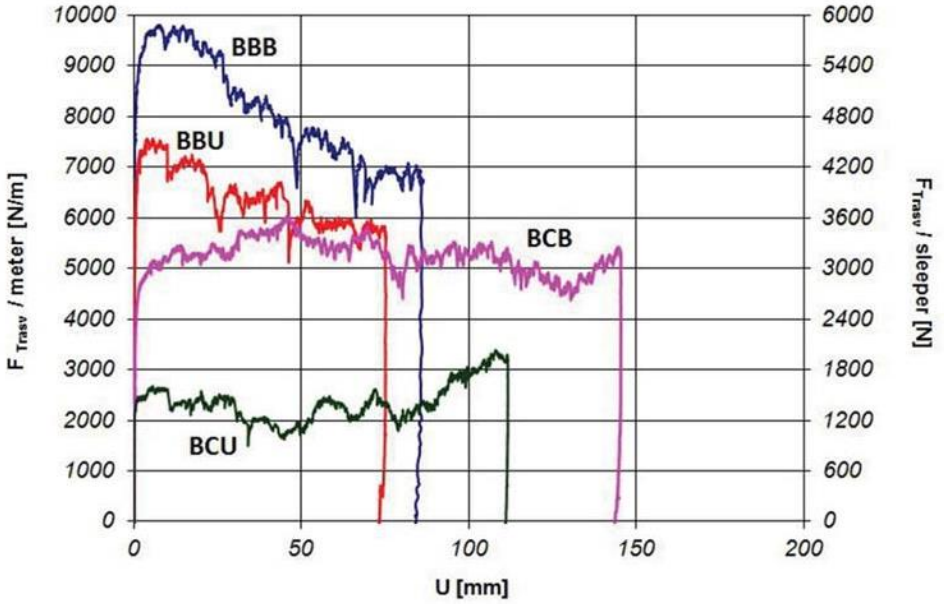

Figure 9. Lateral pull tests: load-displacement curves.

267xl78mm (72 x 72 DPI)

Figure 10. First longitudinal pull test: details of the actuators and their connections to the rails.
FIGURE #10
219x164mm (300 x 300 DPI)

Figure 11. Second longitudinal pull test: detail of actuators linkage to the short track panel.
FIGURE #11
192x89mm (300 x 300 DPI)

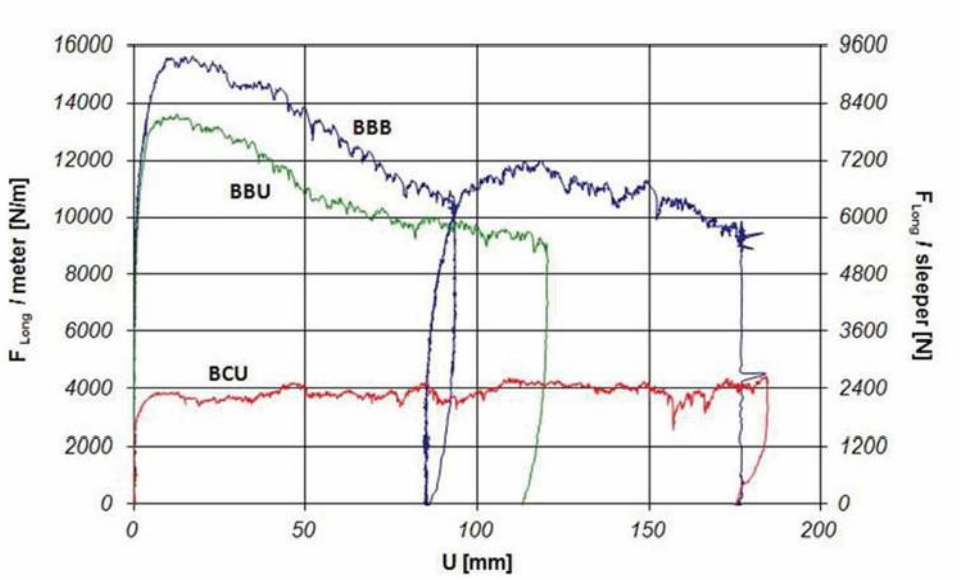

Figure 12. Longitudinal pull tests: load-displacement curves.

257x155mm (72 x 72 DPI)

Table 1. Measured transversal resistance peak values per sleeper (F_{Transv} *Isleeper*) and per track unit length (F_{Transv} *Ilinear metre*).

Scenario	F_{Transv} */sleeper [NJ*	F_{Transv} */lin. metre [N/mJ*
BBB	5879.7	9799.5
BCB	3271.2	5452.0
BBU	4541.4	7569.0
BCU	1599.3	2665.4

Table 2. Contributions of the crib, the shoulder and the under sleeper ballast to the transversal resistance.

Ballast constituents	F_{Transv} ***/sleeper [NJ***	F_{Transv} ***/lin. metre [N/mJ***	***Percentage rates (from BBB, BCB, BCU)***	***Percentage rates (from BBB, BBU, BCU)***	***Average percentage rates***
Base	1599.3	2665.4	27.2 %	27.2 %	**27.2 %**
Between sleepers (BBB-BCB)	2608.5	4347.5	44.4 %		**47.2 %**
Between sleepers (BBU-BCU)	2942.1	4903.5		50.0 %	

Table 3. Measured longitudinal resistance peak values per sleeper (F_{Long} *Isleeper*) and per track unit length (F_{Long} *Ilinear metre*).

Scenario	F_{long} */sleeper [NJ*	F_{long} */lin. metre [N/mJ*
BBB	9385	15641
BBU	8173	13622
BCU	2667	4445

Table 4. Contributions of the crib, the shoulder and the under sleeper ballast to the longitudinal resistance.

Ballast constituents	F_{long} */sleeper [NJ*	F_{long} */lin. metre [N/mJ*	*Percentage rates*
Base	2667	4445	28.4 %
Between sleepers (BBU-BCU)	5506	9176	58.7 %
Shoulder (BBB-BBU)	1212	2020	12.9 %
Total (BBB)	9385	15641	100 %

Table 5. Measured lateral resistances peak values.

Scenario	F_{Transv} */sleeper [NJ*	F_{Transv} */lin. metre [N/mJ*
This study	5879.7	9799.5
RFI 230 h 30 n.c. [9]	5545.0	9241.7
RFI 240 h 30 n.c. [9]	7715.0	12858.3
RFI 240 h 30 c.b.w. [9]	10000.0	16666.6
RFI 240 h 30 c. [9]	8840.0	14733.3

RFI230 / RFI240: type of sleeper
h: height, in cm, of the ballast under sleepers
n.c.: non-consolidated ballast
c.: consolidated ballast;
c.b.w.: consolidated ballast and ballast wall

Table 6. Comparison of the contributions to lateral resistance with those of ERRI [25J and Le Pen and Powrie [30J.

	This study		*ERRI [25J*		***I****e Pen and Powrie [30J*
Ballast constituents	F_{Transv} */sleeper [NJ*	*Percentage rates*	F_{Transv} */sleeper [NJ*	*Percentage rates*	F_{Transv} */sleeper*
Base	1599.3	27.2 %	2900	37 %	$LIVI_{@\ Peak} = 0.55$
Crib	2775.3	47.2 %	2100	27 %	2935 N
Shoulder (55 cm)	1505.1	25.6 %	2800	36 %	2231 N
Total	5879.7	100 %	7800	100 %	

Table 7. Comparison of the contributions to longitudinal resistance with those of ERRI [25J.

	This study		*ERRI [34J*	
Ballast constituents	F_{long} */sleeper [NJ*	*Percentage rates*	F_{lONG} */sleeper [NJ*	*Percentage rates*
Base	2667	28.4 %	3300	36 %
Crib	5506	58.7 %	4600	51 %
Shoulder	1212	12.9 %	1200	13 %
Total	9385	100 %	9100	100 %